J Biomol NMR (2007) 37:65–77
DOI 10.1007/s10858-006-9104-z

ARTICLE

Simultaneous α/β spin-state selection for ^{13}C and ^{15}N from a time-shared HSQC-IPAP experiment

Pau Nolis · Teodor Parella

Received: 1 May 2006 / Accepted: 19 October 2006 / Published online: 12 December 2006

Abstract Two novel HSQC-IPAP approaches are proposed to achieve α/β spin-state editing simultaneously for ^{13}C and ^{15}N in a single NMR experiment. The pulse schemes are based on a time-shared (TS) 2D $^{1}H,^{13}C/^{1}H,^{15}N$-HSQC correlation experiment that combines concatenated echo elements for simultaneous J(CH) and J(NH) coupling constants evolution, TS evolution of ^{13}C and ^{15}N chemical shifts in the indirect dimension and heteronuclear α/β-spin-state selection by means of the IPAP principle. Heteronuclear α/β-editing for all CH_n (n = 1–3) and NH_n (1–2) multiplicities can be achieved in the detected F2 dimension of a single TS-HSQC-F2-IPAP experiment. On the other hand, an alternative TS-HSQC-F1-IPAP experiment is also proposed to achieve α/β-editing in the indirect F1 dimension. Experimental and simulated data is provided to evaluate these principles in terms of sensitivity and performance simultaneously on backbone and side-chain CH, CH_2, CH_3, NH, and NH_2 spin systems in uniformly $^{13}C/^{15}N$-labeled proteins and in small natural-abundance peptides.

Keywords NMR · HSQC · Spin-state selection · Coupling constants · IPAP · Time-sharing

Introduction

Time-shared (TS) evolution of different coherences (Sørensen 1990; Farmer II 1991; Boelens et al. 1994; Mariani et al. 1994; Sattler et al. 1995; Uhrin et al. 2000; Frueh et al. 2005) and reduced-dimensionality (RD) experiments (Szyperski et al. 2002; Kim and Szyperski 2003) have been introduced in high-resolution bio-molecular NMR spectroscopy to provide valuable time savings in data collection. These concepts rely on the joint sampling of independent NMR parameters in indirect evolution times and it has been successfully applied for multiple frequency labeling of several nuclei into the same indirect dimension of multidimensional NMR experiments. One illustrative example is the TS-$^{1}H,^{13}C/^{1}H,^{15}N$-HSQC experiment which allows the simultaneous acquisition of 2D $^{1}H,^{13}C$ and $^{1}H,^{15}N$ correlation HSQC spectra (Sattler et al. 1995). In this experiment, both ^{13}C and ^{15}N chemical shifts evolve simultaneously during the variable t_1 period and therefore all heteronuclear ^{13}C and ^{15}N correlations with the detected ^{1}H can be traced out in the same indirect dimension but from independent spectral widths. It has been recognized that the incorporation of the TS concept in traditional NMR experiments can open new frontiers for structural and dynamic NMR studies. The practical absence of overlapping problems between $^{1}H(N)$ and $^{1}H(C)$ resonances in proteins, the tolerable sensitivity losses associated to additional pulses and longer delays in TS versions compared with regular experiments (Sattler et al. 1995) and the no introduction of considerable extra artifacts makes of the TS approach an attractive NMR tool to speed up data acquisition and to introduce new NMR approaches for further developments into time-consuming higher dimensional triple-resonance or NOESY-edited NMR experiments.

On the other hand, it has been described that several spin-state selective (S^3) coupling patterns, such as

P. Nolis · T. Parella (✉)
Servei de Ressonància Magnètica Nuclear, Facultat de Ciències, Universitat Autònoma de Barcelona, E-08193 Bellaterra, Barcelona, Spain
e-mail: teodor.parella@uab.es

E.COSY, TROSY/anti-TROSY or α/β-editing in the indirect F1- or the detected F2-dimension of 2D correlation experiments based on heteronuclear cross-polarization, can be realized simultaneously for different multiplicities, namely NH/NH_2 or CH/CH_2 spin systems (Parella and Gairí 2004). Here, we expand this idea by proposing two different versions of the TS-HSQC experiment in order to obtain S^3 editing simultaneously for ^{13}C and ^{15}N using the IPAP principle. Thus, two complementary in-phase (IP) and anti-phase (AP) spectra are separately collected and conveniently added/subtracted to provide two different upfield/downfield-multiplet component spectra (Ottiger et al. 1998). Our first proposed experiment relies on the recently described strategy to achieve S^3 for all multiplicities in the acquisition F2 dimension of a sensitivity-enhanced HSQC experiment (Nolis et al. 2006). This TS-HSQC-F2-IPAP pulse scheme involves TS evolution of coupling constants and chemical shifts, sensitivity-enhanced coherence-order-selective transfer schemes for both ^{13}C and ^{15}N, specific-nucleus $^{13}C/^{15}N$-editing, and appropriate combination of complementary IP and AP data to provide α/β-spin-editing simultaneously for all CH_n (n = 1–3) and NH_n (n = 1–2) spin systems in the same experiment. Experimental and simulated data is provided to evaluate these principles on all backbone and side-chain CH, CH_2, CH_3, NH, and NH_2 spin systems in uniformly $^{13}C/^{15}N$-labeled ubiquitin. The second proposed approach offers the possibility to obtain α/β-spin-editing simultaneously for ^{13}C and ^{15}N in the indirect F1 dimension of a TS-HSQC-F1-IPAP experiment that could allow the determination of heteronuclear scalar and/or residual dipolar coupling (RDC) constants without contamination by homonuclear HH couplings (Ottiger et al. 1998; Ding and Gronenborn 2003; Fehér et al. 2003; Kövér and Batta 2004; Ishii et al. 2001) or the measurement of CSA-dipolar cross-correlation (Hall et al. 2003; Hall and Fushman 2003). Experimental data on a natural-abundance peptide (cyclosporine) demonstrate the successful application of this experiment simultaneously on CH/CH_2 and NH/NH_2 spin systems.

Results and discussion

The proposed TS-HSQC-F2-IPAP (Fig. 1A) and TS-HSQC-F1-IPAP (Fig. 1B) pulse schemes are closely related to the original TS-HSQC experiment (Sattler et al. 1995). There are several general features to be highlighted. Basically, two different $^1H/^{13}C$ and $^1H/^{15}N$ magnetization transfer pathways are superimposed within the same radio-frequency pulse scheme in order to minimize undesired effects of additional pulses and longer delays, particularly suffered for ^{13}C. The advantages offered with the TS approach compared to separate acquisition of single-nucleus experiments have already been discussed and carefully evaluated. Theoretically, a sensitivity enhancement per time unit of 41% should be expected individually for ^{13}C and ^{15}N when both data are required. Our experimental data, extracted from TS-HSQC spectra of ubiquitin, are in excellent agreement with the averaged 30–40% and 15–25% sensitivity gains previously reported for ^{15}N and ^{13}C, respectively (Sattler et al. 1995). Both pulse schemes use concatenated heteronuclear spin-echo periods for simultaneous IP-to-AP dephasing or AP-to-IP refocusing of CH and NH coupling constants. In practical terms, these concatenated double-INEPT elements have the same duration as conventional ^1H-^{15}N INEPT periods ($2*\Delta_2$ = 1/2J(NH)~5.5 ms) and therefore the expected sensitivity gains for ^{15}N will be minimally affected. However, in the case of ^{13}C, each concatenated block is about 2 ms longer ($2*\Delta_1$ = 1/4J(CH)~3.5 ms) than the corresponding ^1H-^{13}C INEPT periods and the resulting relaxation losses can explain the more moderate sensitivity gains. Finally, spectral width and resolution in the indirect dimension can be independently set for ^{13}C and ^{15}N because ^{15}N chemical shift evolves during a period $t_1' + t_1$ whereas ^{13}C chemical shift only evolves during the period t_1.

TS-HSQC-F2-IPAP experiment

The proposed TS-HSQC-F2-IPAP experiment can be understood as a sensitivity-enhanced TS-HSQC pulse scheme without heteronuclear decoupling during acquisition (Fig. 1A). Following the first concatenated INEPT block that creates anti-phase proton magnetization with respect to ^{13}C and ^{15}N, the gradient G_4 applied after the $90°_y(^1H)$ pulse acts as a zz-filter and also dephases any residual transverse water magnetization. Although not shown, water-flip back can be also incorporated during the zz filter to get improved water suppression if needed. Then, heteronuclear chemical shift evolution takes place in two consecutive t_1' and t_1 steps. During the initial t_1' period, the transverse ^{15}N magnetization created by the first $90°(^{15}N)$ pulse evolves under the only effect of its chemical shift whereas ^{13}C remains as H_zC_z magnetization. On the other hand, frequency labeling of both ^{13}C and ^{15}N chemical shifts takes place simultaneously during the

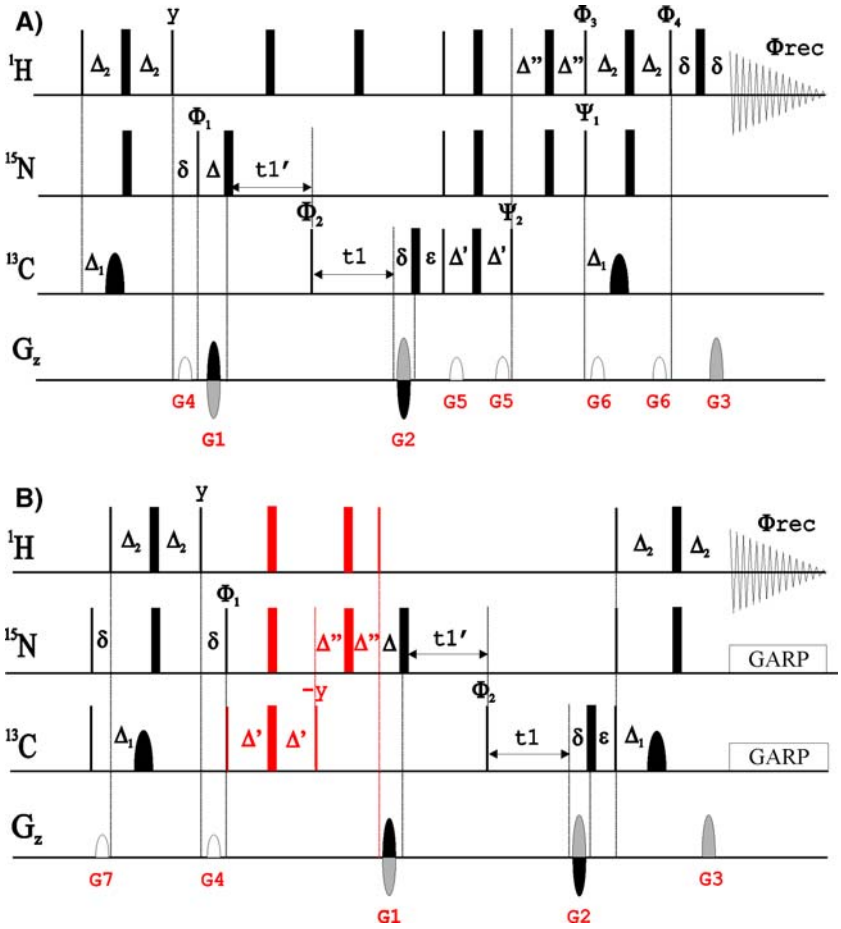

Fig. 1 Schematic representation of the TS-^{1}H,^{13}C/^{1}H,^{15}N—(**A**) HSQC-F2-IPAP and (**B**) HSQC-F1-IPAP experiments. All narrow and wide rectangular pulses are applied with flip angles of 90° and 180° along the *x*-axis unless indicated otherwise. The shaped ^{13}C 180° pulses can be a 500 μs smoothed chirp pulse for broadband inversion or a 256 μs Q3 Gaussian cascade for selective aliphatic inversion. The inter-pulse delays are optimized to $\Delta_1 = 1/4J_{CH}$, $\Delta_2 = 1/4J_{NH}$, $\Delta' = \Delta_1$ and $\Delta'' = \Delta_2 - \Delta'$ for CH and NH multiplicities. On the other hand, Δ' and Δ'' should be set to $\Delta_1/2$ for CH_2-optimized and $\Delta_2/2 - \Delta_1$ for NH_2-optimized, respectively. The periods ε and Δ compensate evolution during the variable t_1 and t_1' periods and the time increments are set to $\Delta t_1 = 1/SW(C)$ and $\Delta t'_1 = 1/SW(N) - 1/SW(C)$. A basic two-step phase cycle is employed: $\phi_1 = \phi_2 = (x, -x)$, $\phi_{rec} = (x, -x)$. ^{15}N cross peaks can be inverted with respect to ^{13}C cross peaks by inverting the phase of the first 90°(N) pulse, $\phi_1 = (-x, x)$. In Fig. B, the initial 90°(C) and 90°(N) pulses and the gradient G7 are applied to avoid recovery of the Boltzmann populations that could produce undesired contributions and multiplet line distortions. All gradients have a sine shape and their durations (δ in ms) and strengths (G/cm) are: G1 = (1 ms, –29.53), G2 = (1 ms, 20.06), G3 = (1 ms, 5.05), G4 = (600 μs, 49.60), G5 = (600 μs, 6.82), G6 = (600 μs, –3.10), G7 = (600 μs, 9.30). (**A**) In TS-HSQC-F2-IPAP experiments, α-edited and β-edited spectra are generated by addition/subtraction of in-phase (IP) and anti-phase (AP) data separately collected as a function of phases ϕ_3 and ϕ_4: (i) HSQC-IP(*y*): ($\phi_3 = y$, $\phi_4 = x$); (ii) HSQC-AP(*y*): ($\phi_3 = x$, $\phi_4 = y$). Frequency discrimination in F1 was achieved using sensitivity-enhanced gradient selection. The echo and anti-echo signals were collected separately by inverting the sign of gradients G1 and G2 together with the inversion of ψ_1 (=–*y*) and ψ_2 (=*y*). (**B**) In TS-HSQC-F1-IPAP experiments, α-edited and β-edited spectra are generated by addition/subtraction of in-phase (IP) and anti-phase (AP) data separately collected without and with the pulses marked in red, respectively. Frequency discrimination in F1 was achieved using gradient selection. The echo and anti-echo signals were collected separately by inverting the sign of G1 and G2 gradients

subsequent t_1 period. The dephasing gradient strengths G_1 and G_2 are conveniently adjusted as a function of these available transverse coherences. The following concatenated retro-INEPT blocks refocus anti-phase ^{13}C and ^{15}N magnetization in a manner that increases the sensitivity for both nuclei thanks to the PEP approach (Kay et al. 1992; Schleucher et al. 1994) whereas the gradient pairs G_5 and G_6 remove artifacts associated with imperfect 180° pulses. Finally, observable proton magnetization is rephased by the gradient G_3 (the ratio between G_1:G_2:G_3 is –6:4:1) and acquisition is performed without heteronuclear ^{13}C/^{15}N decoupling in order to achieve the corresponding IP and AP spectra as a function of the phases ϕ_3 and ϕ_4 (Nolis et al. 2006). Sensitivity-enhanced α- and β-edited TS-HSQC sub-spectra are generated by addition/

subtraction of complementary in-phase (IP(y): $\phi_3 = y$, $\phi_4 = x$, $\psi_1 = -y$, $\psi_2 = y$) and anti-phase (AP(y): $\phi_3 = x$, $\phi_4 = y$, $\psi_1 = -y$, $\psi_2 = y$) data. Although not strictly necessary because α/β-editing is achieved in the acquisition F2 dimension, further enhancements could be introduced in the indirect F1 dimension when applied specifically on ^{13}C-labeled compounds such as, for instance, spectral aliasing, selective ^{13}CO decoupling during t_1 or implementation of combined constant-time (CT) ^{13}C and variable-time (VT) ^{15}N chemical shift labeling periods (Uhrin et al. 2000).

To avoid confusion during spectral analysis and without sensitivity penalties, the phase of cross-peaks correlating amide proton and nitrogen coherences can optionally be inverted by means of the first 90° ^{15}N pulse ($\phi_1 = x$ or $-x$). In practice and as clearly shown from simulated data (Fig. 2), four separate data can be recorded in an interleaved manner by inverting ϕ_1 and ϕ_3/ϕ_4 (A–D in Fig. 2) and properly combined to afford four individual α/^{13}C-, β/^{13}C-, α/^{15}N-, β/^{15}N-edited HSQC spectra with optimum sensitivity (E–H in Fig. 2). For experimental verification, TS-HSQC-F2-IPAP data were recorded on uniformly ^{13}C/^{15}N-labeled ubiquitin to yield clean and simplified spectra with excellent solvent suppression (Fig. 3). The main S^3 features of this approach are more visible from the different expanded regions of the same spectra (Fig. 4) that are suitable for the measurement of coupling constants involving all CH_n and NH_n spin systems.

The key topics of this IPAP strategy already discussed in regular sensitivity-improved HSQC-IPAP experiments (Nolis et al. 2006), that includes overall transfer efficiencies, inter-pulse delay optimization, setting of pulse phases or percentage of undesired cross-talk present for any type of multiplicity, can be applied to the proposed scheme of Fig. 1A. For in-

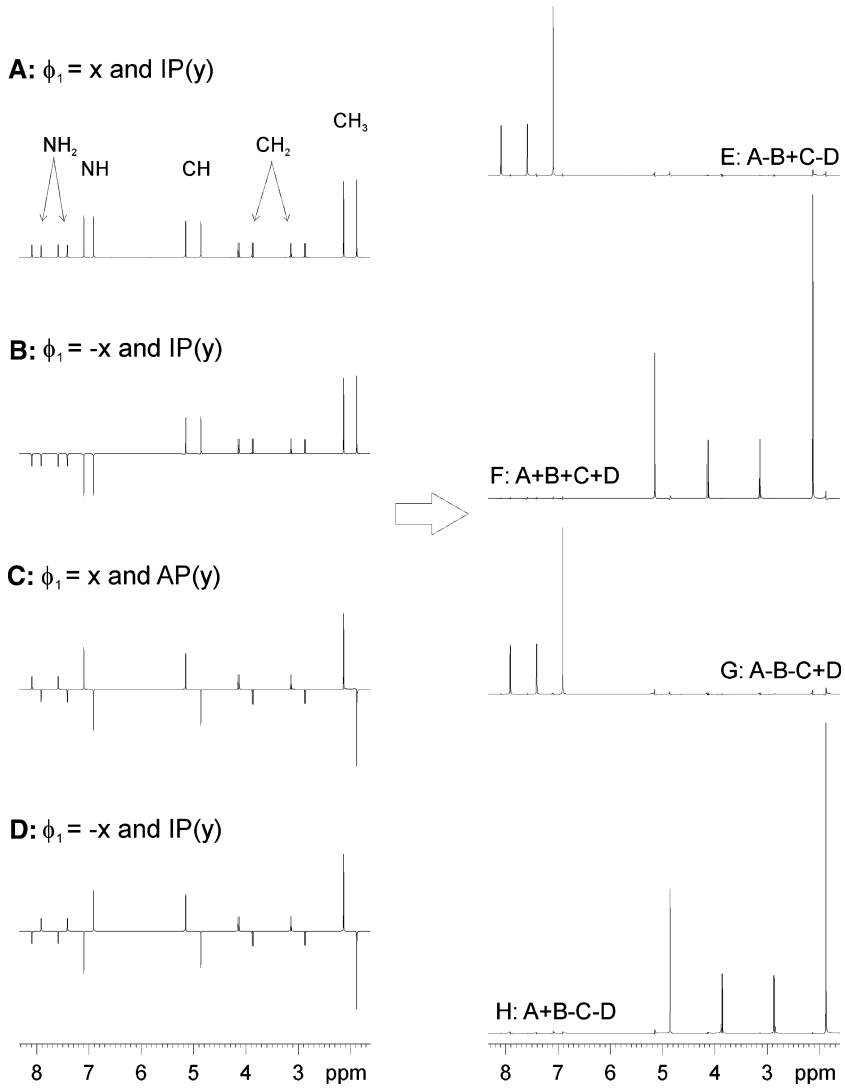

Fig. 2 Simulated 1D TS-HSQC-IPAP spectra showing the schematic data acquisition/processing strategy designed to achieve simultaneous spin-state (IP(y) with $\phi_3 = y$ and $\phi_4 = x$; or AP(y) with $\phi_3 = x$ and $\phi_4 = y$) and nucleus ($\phi_1 = x$ or $-x$) editing for all CH_n and NH_n multiplicities. Four data are collected (**A**, **B**, **C**, **D**) and combined (**E**, **F**, **G**, **H**) accordingly. Spin system used in the simulation: CH ($\delta(^1H) = 5$ ppm, $\delta(^{13}C) = 55$ ppm, $^1J_{CH} = 145$ Hz); CH_2 ($\delta(^1H) = 3$ and 4 ppm, $\delta(^{13}C) = 30$ ppm, $^1J_{CH} = 135$ Hz; $^2J_{HH} = 10$ Hz); CH_3 ($\delta(^1H) = 2$ ppm, $\delta(^{13}C) = 20$ ppm, $^1J_{CH} = 125$ Hz); NH ($\delta(^1H) = 7$ ppm, $\delta(^{15}N) = 115$ ppm, $^1J_{NH} = 90$ Hz); NH_2 ($\delta(^1H) = 7.5$ and 8 ppm, $\delta(^{15}N) = 105$ ppm, $^1J_{NH} = 90$ Hz; $^2J_{HH} = 2$ Hz)

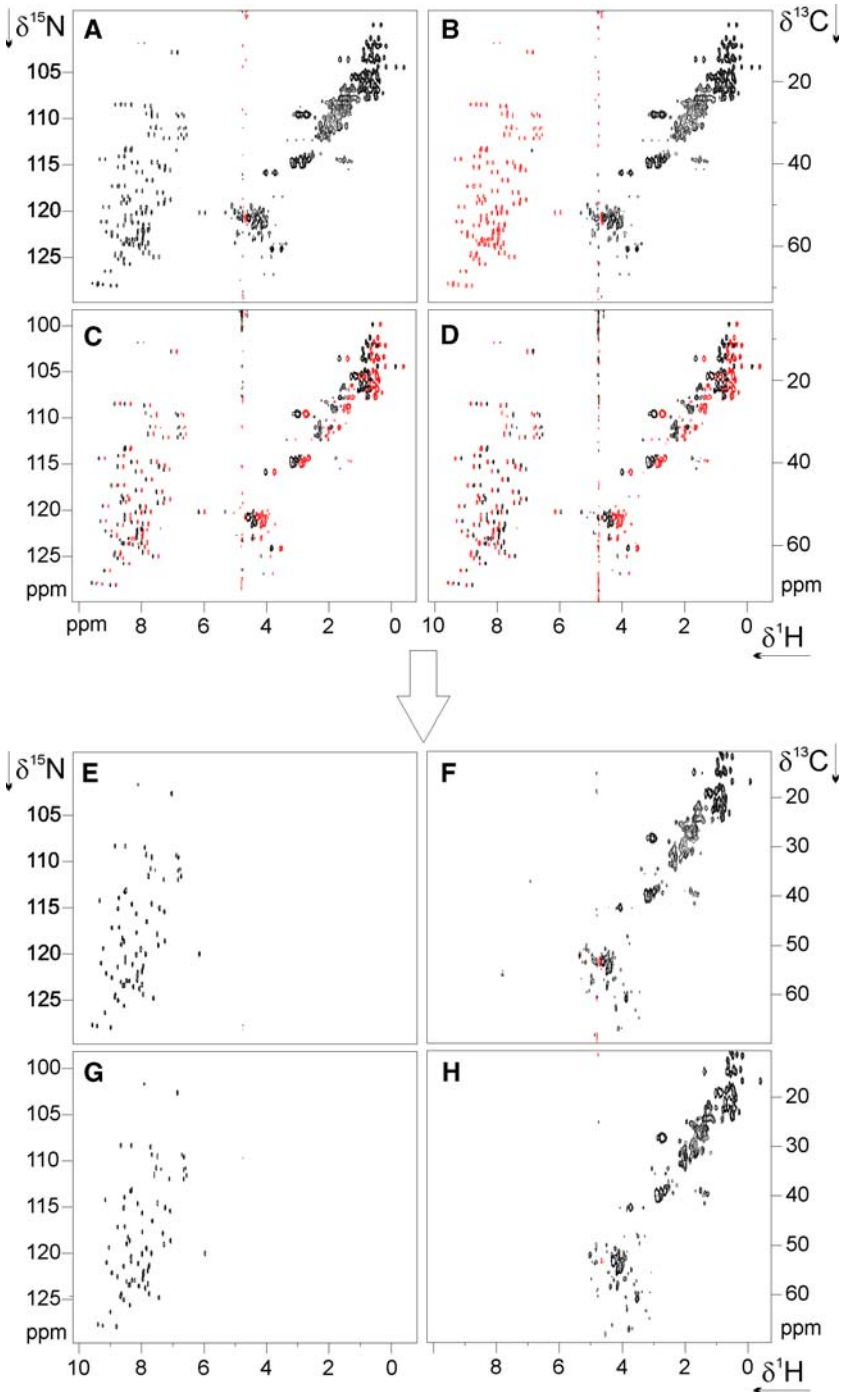

Fig. 3 Experimental 2D TS-^{1}H,^{13}C/^{1}H,^{15}N-HSQC-F2-IPAP spectra of uniformly ^{13}C/^{15}N-labeled ubiquitin. The original time-domain data (**A**–**D**) were conveniently combined and processed as described in Fig. 2 to yield separate (**F** and **H**) α/β-edited ^{1}H,^{13}C and (**E** and **G**) α/β-edited ^{1}H,^{15}N HSQC maps

stance, the presence of undesired cross-talks when different coupling values are present have been evaluated from simulated data on NH and CH spin systems (Fig. 5). It is clear that excellent results are obtained into a range of ΔJ(CH) and ΔJ(NH) about ±30%. It was also reported that cross-talk is much more sensitive for CH_2 and NH_2 spin systems but good results are still obtained into a range of ΔJ(XH) = ±15%. According to this theoretical predictions, experimental data fully confirm the excellent tolerance to cross-talk for all multiplicities in a wide range of coupling values. In Fig. 6 it can be seen that practically cross talk is below 2% in a complete range of 120–160 Hz for J(CH) and 70–110 Hz for J(NH) and for all CH_n and NH_n multiplicities.

As described in our previous work (Nolis et al. 2006), analogue TS-HSQC-F2-IPAP sub-spectra obtained from addition/subtraction of complementary IP(x)

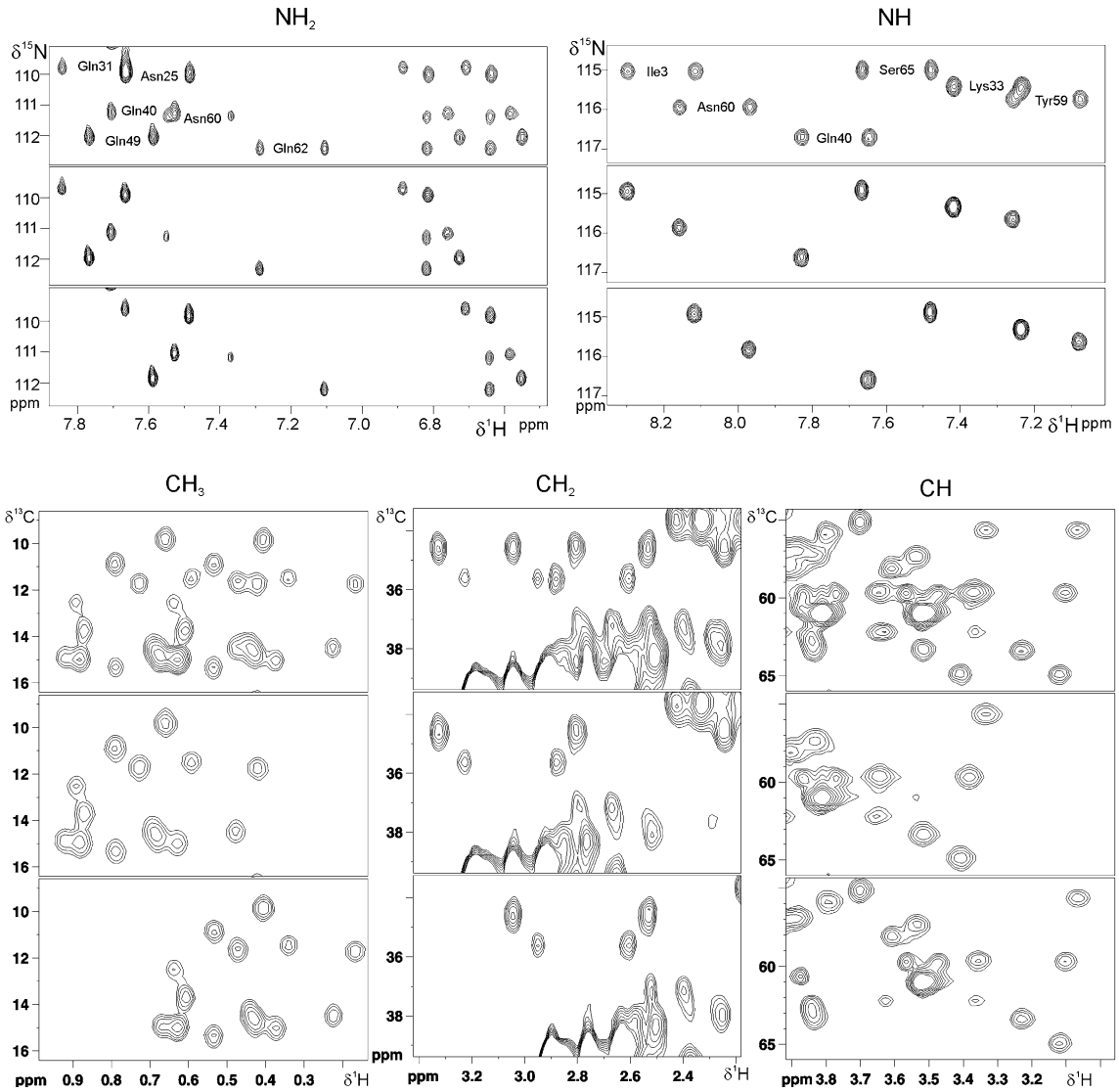

Fig. 4 Selected expanded areas extracted from the 2D TS-HSQC-F2-IPAP spectra of Fig. 3 (**E**–**H**) showing the clean and simultaneous α/β-editing achieved for all NH, NH_2, CH, CH_2 and CH_3. The same region of the F2 fully-coupled IP(y) spectrum (top) is also shown for comparison in each expansion

($\phi_3 = y$, $\phi_4 = x$, $\psi_1 = \psi_2 = x$) and AP(x) ($\phi_3 = x$, $\phi_4 = y$, $\psi_1 = \psi_2 = x$) data could be used to measure simultaneously all $^1J_{CH}$ ($^1D_{CH}$) and $^1J_{NH}$ ($^1D_{NH}$) coupling values for all multiplicities and also the geminal $^2J_{HH}$ ($^2D_{HH}$) in NH_2 and CH_2 groups via the analysis of DQ/ZQ (Permi 2002; Nolis et al. 2006) or multiplet-line-selective (Carlomagno et al. 2000; Miclet et al. 2003, 2004) coupling patterns. Eight complementary data can be acquired in an interleaved way as a function of phases ϕ_1/ϕ_2 (nucleus editing), ϕ_3/ϕ_4 (α/β-editing: IP or AP) and ψ_1/ψ_2 (set to x or $-x$, to generate DQ ($^1J_{XH}+^2J_{HH}$) or ZQ ($^1J_{XH}-^2J_{HH}$) doublet patterns for XH_2 groups, respectively) (Fig. 7) and further processed to afford eight simplified S^3 spectra accordingly to simple linear combinations. Experimental 1D slice taken for different CH_2 and NH_2 groups in the 2D TS-HSQC-IPAP spectra of ubiquitin shows excellent line selection for all multiplicities (Fig. 8).

It is worth to say that the sensitivity of ^{13}C signals in the proposed TS experiment will depend on the required resolution in the ^{15}N dimension that will be defined by the maximum value of the variable t_1' period, t_1' (max). For this reason, a compromise value between the maximum t_1' value and the spectral width in the N dimension is required. On the other hand, the use of PEP can restrict the utility to small peptides and or proteins below molecular weight of 10–15 kDa due to short relaxation times for ^{13}C. Cross-correlation

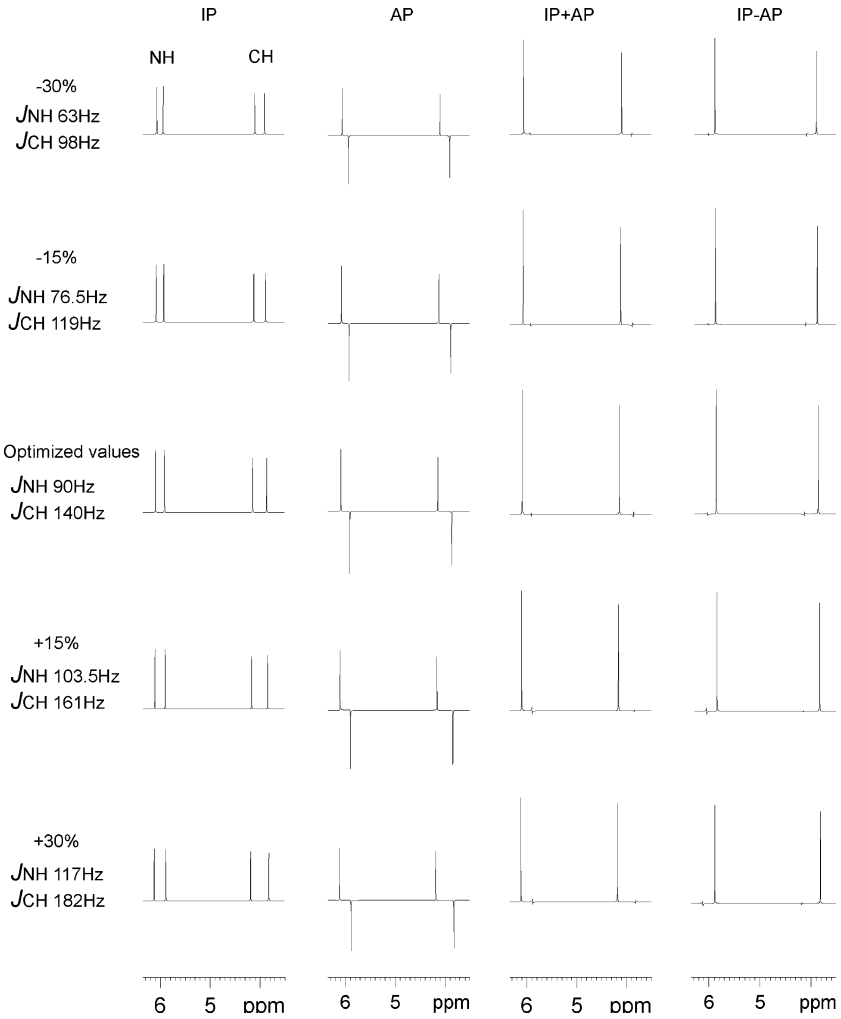

Fig. 5 Effectiveness of the α/β-spin editing encoding and presence of cross-talk for two isolated NH and CH spin systems in a range of $\Delta J = \pm 30\%$. $^{1}J_{CH}$ and $^{1}J_{NH}$ values were varied as described in each row. All simulated 1D TS-HSQC spectra were optimized to $\Delta_1 = 1.8$ ms ($^{1}J(CH) = 140$ Hz) and $\Delta_2 = 2.7$ ms ($^{1}J(NH) = 90$ Hz) and with the following phases: $\phi_1 = x$, $\phi_2 = x$, $\psi_1 = -y$, $\psi_2 = y$. IP and AP data were generated using $\phi_3 = y$, $\phi_4 = x$ and $\phi_3 = x$, $\phi_4 = y$, respectively

effects could also produce non-complementary IP and AP data and cross-talks could be more prominent in such cases. The use of different scaling k factors when process IP ± k*AP data could be a good post-processing practice to minimize such artifacts if they are present.

TS-HSQC-F1-IPAP experiment

The TS-HSQC-F1-IPAP experiment (Fig. 1B) is another variant of the regular TS-HSQC pulse sequence in which evolution of both heteronuclear CH and NH couplings take place simultaneously during the variable t_1' and t_1 periods because decoupling 180°(^{1}H) pulses are not applied. The advantage to measure heteronuclear J(CH) and J(NH) from the indirect dimension of the HSQC map relies on the absence of proton–proton coupling splittings. Whereas the IP spectrum is just a F1-coupled TS-HSQC experiment, the AP counterpart employs an additional refocusing period just prior to the t_1' period (see pulses and delays marked in red in Fig. 1B) in an analogue way as reported in the original HSQC-IPAP sequence (Ottiger et al. 1998). For IS spin systems, the AP building block works as follows: After the application of simultaneous 90°$_x$(^{13}C) and 90°$_x$(^{15}N) pulses, antiphase ^{15}N and ^{13}C magnetizations are modulated during the double heteronuclear and concatenated echo. At the end of the Δ'(=1/4JCH)) period, in-phase C_x magnetization is stored as C_z magnetization by a 90°$_{-y}$(^{13}C) pulse whereas J(NH) continues evolving during an additional $\Delta'' = \Delta_2 - \Delta'$ delay up to achieve in-phase N_x magnetization. After this, ^{15}N chemical shift and J(NH) evolves during the free evolution t_1' period whereas ^{13}C is retained at $+z$ axis. The gradient G1 labels transverse ^{15}N coherence and also acts as a purge gradient for ^{13}C magnetization. Transverse ^{13}C magnetization is then created by a 90°(^{13}C) pulse and during the t_1 period, all J(CH), J(NH), δ(^{15}N) and δ(^{13}C) components evolve freely to create a mixture of

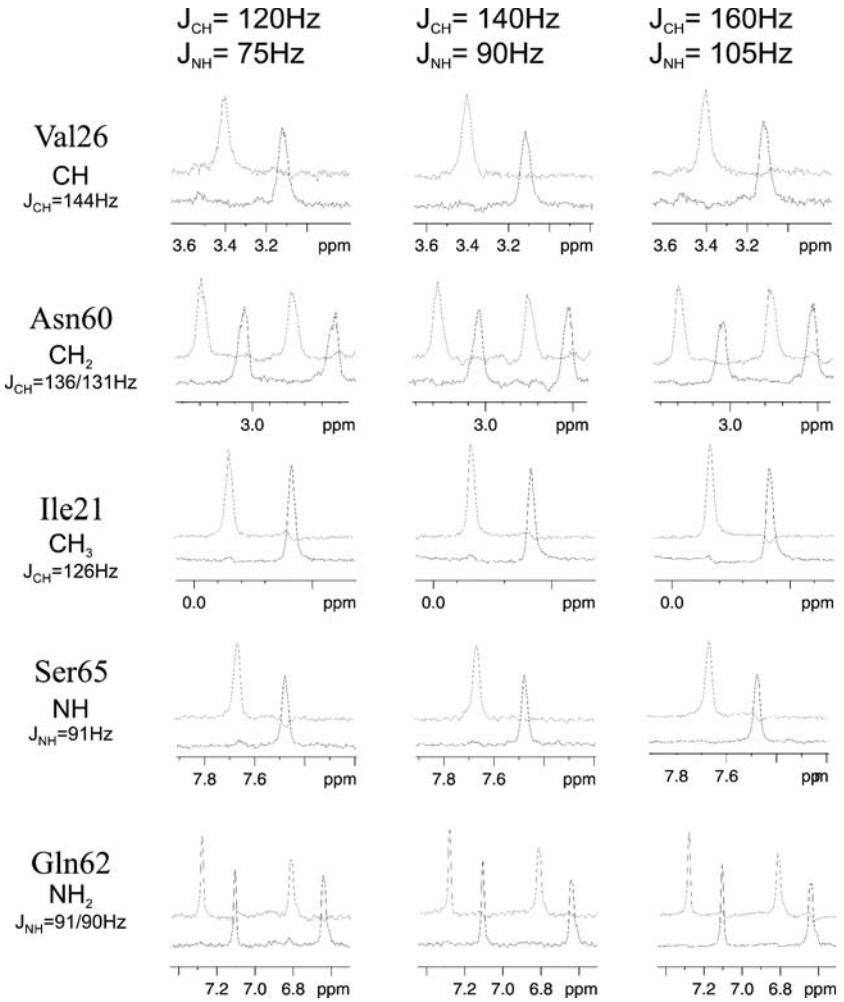

Fig. 6 1D slices extracted from F2-IPAP TS-HSQC spectra of ubiquitin showing the excellent behaviour of α/β editing and absence of cross-talk for all multiplicities in a considerable range of coupling constant values. Spectra were recorded as described in experimental section with the inter-pulse periods optimized to the J(CH) and J(NH) values shown in top of each column. The experimental J(CH) and J(NH) values for each target multiplicity are also included in each row

in-phase and anti-phase ^{13}C and ^{15}N coherences which are labeled with the G2 gradient. Then, ^{13}C and ^{15}N magnetization are back converted to detectable ^{1}H magnetization by a concatenated INEPT transfer and coherence selection is achieved using a gradient G1:G2:G3 ratio of –6:4:1. Finally, proton acquisition is performed with simultaneous ^{13}C and ^{15}N decoupling to ensure that heteronuclear couplings do not appear in the acquisition dimension. The F1-IPAP sequence in Fig. 1B has a reduced sensitivity compared to the F2-IPAP experiment since PEP is not applied. However, the sensitivity gain ratios when compared TS versus standard F1-IPAP sequences will remain the same, about a factor of 1.41.

Figure 9 shows expanded regions of the acquired 2D IP and AP and the resulting α- and β-edited TS-HSQC spectra of cyclosporine in which clean spin-state editing is achieved simultaneously for all CH and NH groups. As predicted theoretically, the experimental sensitivity gains per time unit for ^{15}N are about +30/+40% mainly because the duration of each concatenated block in the TS version is the same (optimized to 1/2J(NH)) than in the original ^{15}N-HSQC-IPAP pulse sequence. However, the poorer sensitivities gains achieved for ^{13}C (between +15% and +25%) can be attributed to relaxation of ^{13}C zz magnetization during the t_1' period in the AP experiment and also to additional ^{13}C T_2 relaxation during the longer concatenated INEPT steps.

The features for measuring scalar and/or RDC constants from the indirect dimension of TS-HSQC-F1-IPAP spectra are analogous to the original HSQC-IPAP experiment (Ottiger et al. 1998). As a major drawbacks, the measured splitting will depend somewhat on the linewidth, the quality of CH correlations for large protein can be degraded by an extensive overlap in the carbon dispersed region and, in addition, a number of H^{α} proton resonances could be covered by the residual water signal. Furthermore, differences on signal intensities between IP and AP data can be attributed to differential relaxation properties, non-

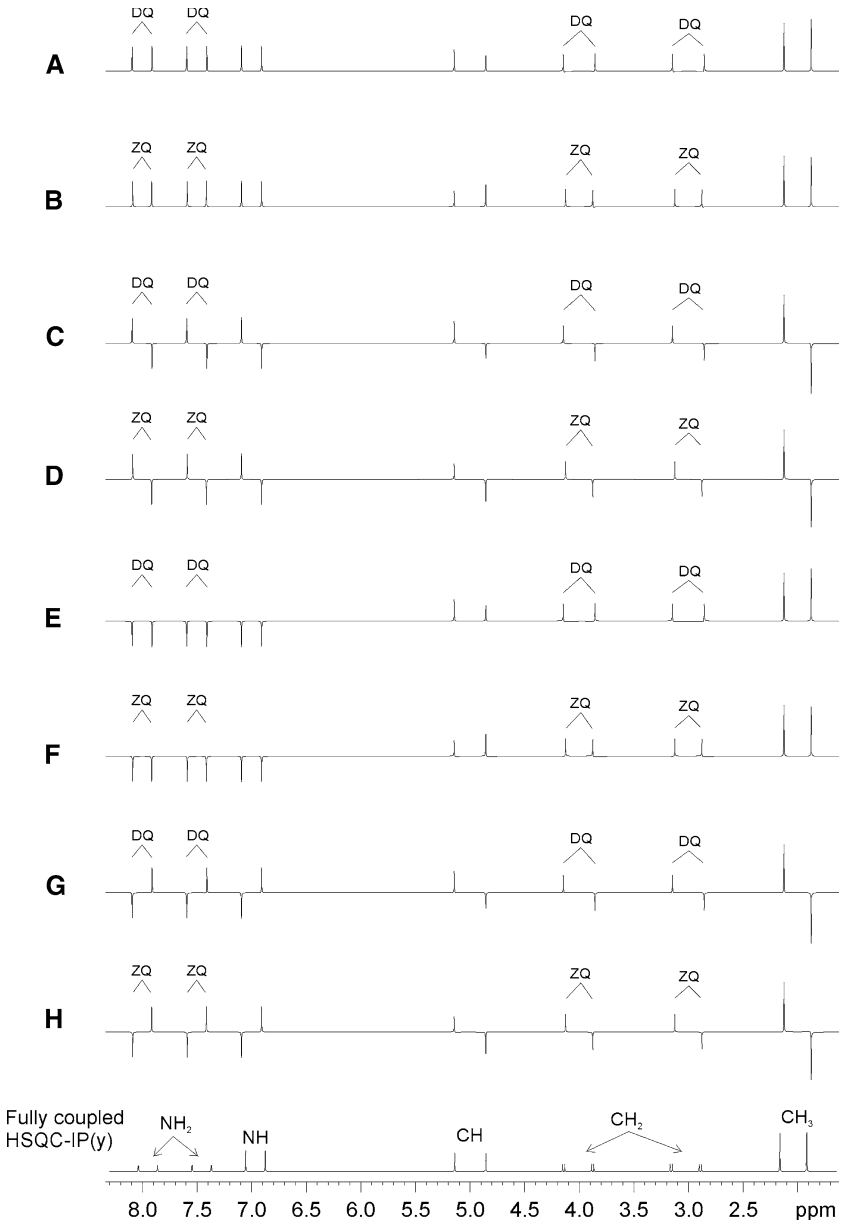

Fig. 7 Schematic representation of the strategy followed for data acquisition in IP(x) and AP(x) experiments. Eight separated TS-HSQC data were simulated as a function of the phases ϕ_1/ϕ_2 (nucleus editing), ϕ_3/ϕ_4 (IP or AP editing) and ψ_1/ψ_2 (DQ/ZQ editing for I_2S groups). (**A**) $\phi_1 = x$, $\phi_2 = x$, $\phi_3 = y$, $\phi_4 = x$, $\psi_1 = x$, $\psi_2 = -x$; (**B**) $\phi_1 = x$, $\phi_2 = x$, $\phi_3 = y$, $\phi_4 = x$, $\psi_1 = -x$, $\psi_2 = x$; (**C**) $\phi_1 = x$, $\phi_2 = x$, $\phi_3 = x$, $\phi_4 = y$, $\psi_1 = x$, $\psi_2 = -x$; (**D**) $\phi_1 = x$, $\phi_2 = x$, $\phi_3 = x$, $\phi_4 = y$, $\psi_1 = -x$, $\psi_2 = x$; (**E**) $\phi_1 = -x$, $\phi_2 = x$, $\phi_3 = y$, $\phi_4 = x$, $\psi_1 = x$, $\psi_2 = -x$; (**F**) $\phi_1 = -x$, $\phi_2 = x$, $\phi_3 = y$, $\phi_4 = x$, $\psi_1 = -x$, $\psi_2 = x$; (**G**) $\phi_1 = -x$, $\phi_2 = x$, $\phi_3 = x$, $\phi_4 = y$, $\psi_1 = x$, $\psi_2 = -x$; (**H**) $\phi_1 = -x$, $\phi_2 = x$, $\phi_3 = x$, $\phi_4 = y$, $\psi_1 = -x$, $\psi_2 = x$. The same spin system definition as Fig. 2 was used. Linear combination of these eight acquired afford eight separated multiplet-line selective spectra as shown in Fig. 8

optimal optimization of inter-pulse delays or off-resonance mismatch effects. In practice, the use of different scaling factors (k) when IP and AP data are combined can minimize undesired cross-talk. In the case of cyclosporine, experimental k values of 1 and 1.1 yields clean S^3 editing for NH and CH, respectively (Fig. 9). On the other hand, it is interesting to note that signals intensities of CH_2 and NH_2 systems strongly depend on the length of the refocused INEPT period. Thus, the resonance lines from XH_2 and XH_3 groups disappear from the spectra in typical experiments optimized to achieve maximum intensity for XH (Δ' and/or Δ'' adjusted to 1/4J). On the other hand, spin-selection for CH_2 and NH_2 can be achieved when AP data is acquired with $\Delta' = \Delta_1/2 = 1/8J(CH)$ and $\Delta'' = \Delta_2/2 - \Delta' = 1/8J(NH)$, respectively (Fig. 10). Under these conditions, spin-selection is also achieved for CH and NH but at expense of some sensitivity attenuation. Unfortunately, the proposed experiment fails for CH_3 groups but a particular solution was previously reported to generate four separate single-component spectra (Kontaxis and Bax 2001).

When working with ^{13}C labeled compounds, constant-time evolution in the ^{13}C dimension could be used to avoid J(CC) splitting in the indirect dimension and to simplify the spectra at expense of some sensitivity loss due to ^{13}C relaxation. In this case, the last 90°(^{15}N) pulse could be moved at the end of t_1' period,

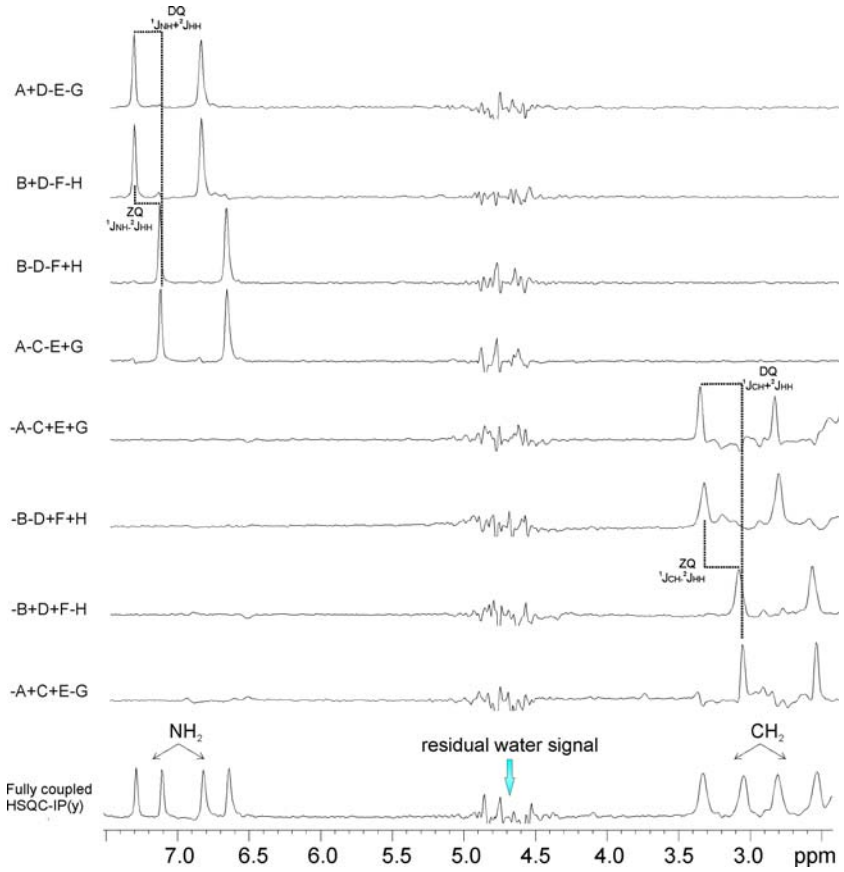

Fig. 8 Experimental data showing homonuclear and heteronuclear αα/αβ/βα/ββ spin-selection on CH_2 and NH_2 spin systems. Each 1D row (corresponding to $\delta^{13}C$ = 34.3 ppm (Asn–60) and $\delta^{15}N$ = 114.4 ppm (Gln-62)) was extracted from the corresponding 2D spectra resulting of the suitable combination of different eight 2D TS-HSQC data acquired as described in Fig. 7 and with the same experimental conditions as Fig. 3. The measured coupling values for the selected signals are $^1J_{CH}$ = 135.9 Hz and 131.6 Hz, $^1J_{NH}$ = 90.9 Hz and 89.5 Hz, $^2J_{HH}(C)$ = 12.4 Hz and $^2J_{HH}(N)$ = 2.1 Hz. At the bottom, the selected row extracted from the F2-coupled 2D TS-HSQC-IP(*y*) experiment is also shown for comparison. Note the practical absence of undesired cross-talk

just prior to the t_1 period, without affect the overall sensitivity of the experiment. In this way, ^{13}C and ^{15}N could be stored as zz magnetization in the IP experiment, and as z and zz magnetization in the AP experiment during the periods t_1' and t_1, respectively. Practicalities to measure $J(C^{\alpha}H^{\alpha})$ coupling values in selectively isotopically enriched proteins in backbone ^{15}N and ^{13}CA, ^{13}CO atoms using the ^1H-^{13}C HSQC-IPAP experiment has been described (Giesen et al. 2001).

Material and experiments

NMR data sets in this work were recorded at 25°C using a Bruker Avance 500 MHz NMR spectrometer equipped with a 5 mm TCI $^1H/^{13}C/^{15}N$ cryoprobe. All data were acquired and processed using TOPSPIN v1.3 (Bruker Biospin, Germany).

The 2D TS-HSQC-F2-IPAP pulse scheme (Fig. 1A) was applied on an uniformly ^{13}C and ^{15}N-labeled ubiquitin sample (concentration of 1.1 mM dissolved in 90% H_2O/10% D_2O). The experimental conditions were as follows: pre-scan delay of 1 s; inter-pulse delays of $\Delta_1 = 1/4J_{CH}$ = 1.72 ms (140 Hz for ^{13}C), $\Delta_2 = 1/4J_{NH}$ = 2.77 ms (90 Hz for ^{15}N), $\Delta' = \Delta_1/2$ = 0.86 ms (optimized to $1/8J_{CH}$ for all carbon multiplicities) and $\Delta'' = \Delta_2 - \Delta'$ = 1.91 ms (optimized to 1/4JNH for NH spin systems); δ = 4 μs + gradient + field recovery delay = 1204 μs; $\varepsilon = \delta + t_1(0)*2 +$ pw(180°–^{13}C) + pw(180°–^1H); $\Delta = 2\varepsilon + t_1(0)*2$ + pw(180°–^{15}N) + pw(180°–^1H) + pw(90°–13C). For each 2D spectrum, $128(t_1)*2K(t_2)$ complex points with 4 scans and acquisition t_{1max} and $t_1'_{max}$ times of 6.36 ms (F_1,C) and 29.95 ms (F_1,N), respectively, were accumulated in about 10 min. Frequency discrimination in F1 was obtained using sensitivity-enhanced gradient selection. After linear prediction and zero-filling in the indirect dimension, a final spectrum consisting of $256(F_1)*2K(F_2)$ real points was obtained. The original time-domain data were conveniently combined and processed as described in Fig. 2 to yield separate α/β-F2-edited ^1H,^{13}C and ^1H,^{15}N HSQC maps as shown in (E–H).

The 2D TS-HSQC-F1-IPAP pulse scheme (Fig. 1B) was applied on a natural-abundance 50 mM cyclosporine sample dissolved in deuterated benzene. The experimental conditions were as follows: pre-scan

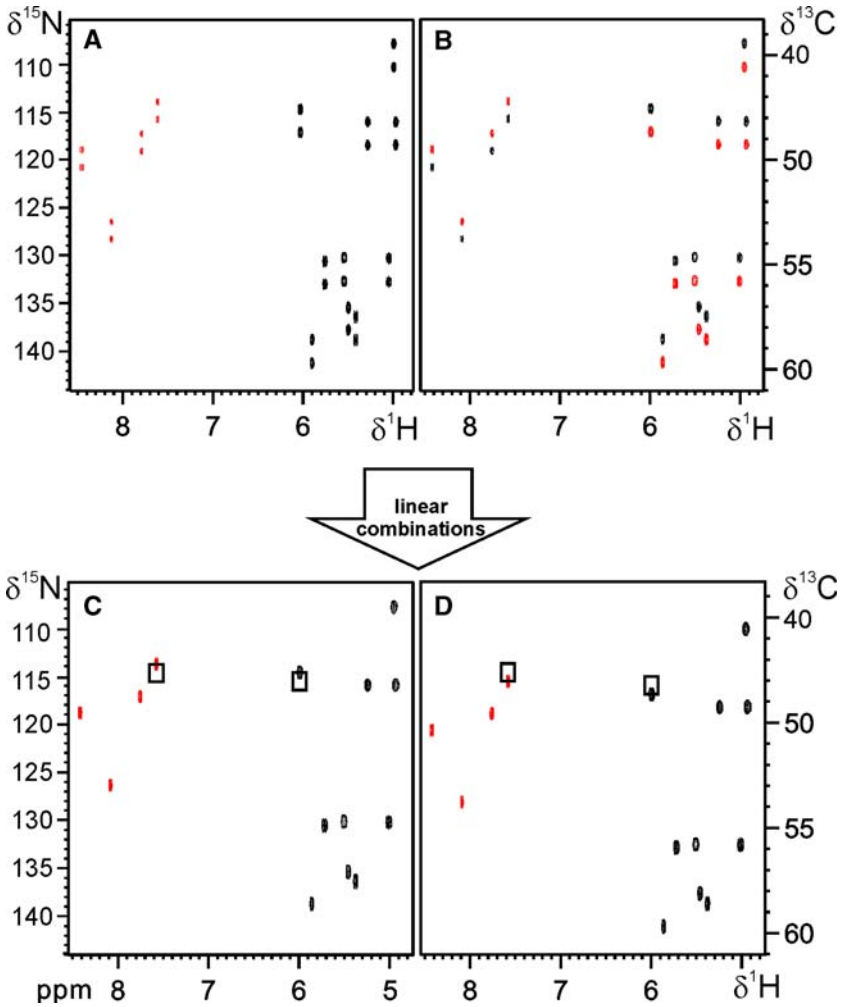

Fig. 9 (**A**) IP and (**B**) AP TS-HSQC spectra of cyclosporine acquired with the sequence of Fig. 1B. The phase of the first ^{15}N 90° pulse was set to $-x$ to invert the corresponding NH resonances with respect to the CH resonances. (**C, D**) Separate F1 spin-state-selective HSQC-IPAP spectra obtained after IP ± AP data combination

delay of 0.7 s; inter-pulse Δ_1 and Δ_2 delays optimized at 140 Hz for CH (1.72 ms) and 90 Hz for NH (2.77 ms), respectively; δ = 4 μs + gradient + field recovery delay = 1204 μs; $\varepsilon = \delta + t_1(0)*2 = 1.21$ ms; $\Delta = 2\varepsilon + t_1'(0)*2 + pw(90°_{-}{}^{13}C) + pw(180°_{-}{}^{13}C) = 2.47$ ms. For each 2D spectrum, $128(t_1)*2K(t_2)$ complex points with 8 scans and acquisition t_{1max} and $t_1'_{max}$ times of 18.5 ms (F_1,C) and 4.5 ms (F_1,N), respectively, were accumulated in about 15 min. Frequency discrimination in F1 was obtained using sensitivity-enhanced gradient selection. After linear prediction and zero-filling in the indirect dimension, a final spectrum consisting of $512(F_1)*2K(F_2)$ real points was obtained. The original time-domain IP and AP data were conveniently combined and processed to yield separate α/β-F1-edited ^{1}H,^{13}C and ^{1}H,^{15}N HSQC maps.

1D spectra were simulated using the program NMR-SIM (Bruker-Biospin AG) and the pulse sequence of Fig. 1A with $t_1 = t_1' = 0$. General simulation conditions: Basic frequency of 500 MHz, carrier frequencies at 5 ppm (^{1}H), 55 ppm (^{13}C), and 110 ppm (^{15}N) and inter-pulse delays set to Δ_1 = 1.8 ms (optimized to $^1J(CH)$ = 138.9 Hz) and Δ_2 = 2.7 ms (optimized to $^1J(CH)$ = 92.6 Hz). Spin system definition used in Figs. 2 and 7: CH ($\delta(^1H)$ = 5 ppm, $\delta(^{13}C)$ = 55 ppm, $^1J_{CH}$ = 145 Hz); CH_2 ($\delta(^1H)$ = 3 and 4 ppm, $\delta(^{13}C)$ = 30 ppm, $^1J_{CH}$ = 135 Hz; $^2J_{HH}$=10 Hz); CH_3 ($\delta(^1H)$ = 2 ppm, $\delta(^{13}C)$ = 20 ppm, $^1J_{CH}$ = 125 Hz); NH ($\delta(^1H)$ = 7 ppm, $\delta(^{15}N)$ = 115 ppm, $^1J_{NH}$ = 90 Hz); NH_2 ($\delta(^1H)$ = 7.5 and 8 ppm, $\delta(^{15}N)$ = 105 ppm, $^1J_{NH}$ = 90 Hz; $^2J_{HH}$ = 2 Hz). Spin system definition used in Fig. 5: CH ($\delta(^1H)$ = 4 ppm, $\delta(^{13}C)$ = 55 ppm); NH ($\delta(^1H)$ = 6 ppm, $\delta(^{15}N)$ = 110 ppm). In Fig. 5, $^1J_{CH}$ and $^1J_{NH}$ values were varied as described in each row.

Conclusions

Often, most of the existing spin-state edited NMR methods are optimal only for a particular multiplicity

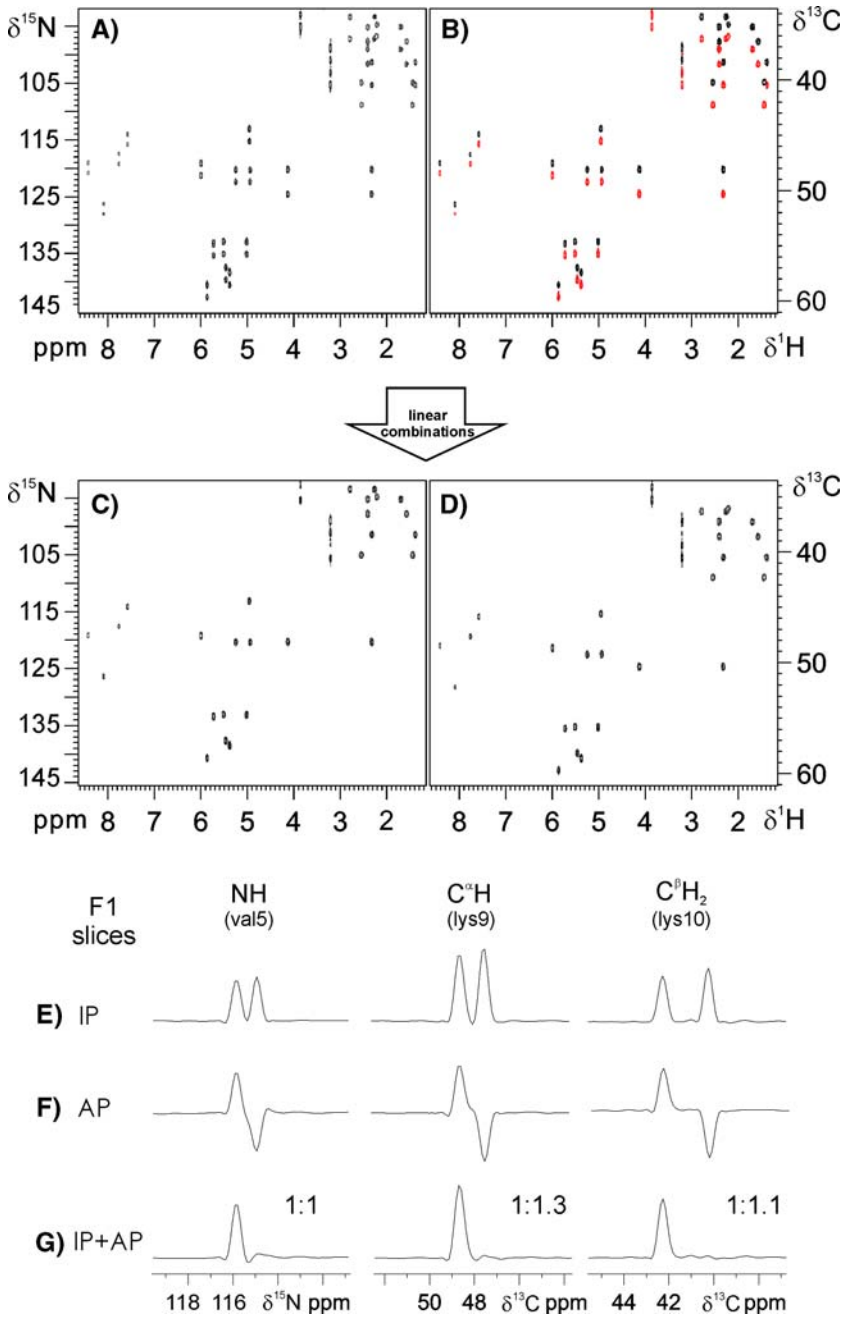

Fig. 10 (**A**, **B**) TS-HSQC-F1-IPAP spectra of cyclosporine optimized for CH_2 spin systems (the delay$\Delta' = \Delta_1/2$ was optimized to 1/8J(CH)) in order to observe spin editing simultaneously for CH, CH_2 and NH spin systems in the resulting α,β-edited spectra shown in (**C**, **D**). Although sensitivity of CH resonances are partially attenuated with respect to an experiment specifically optimized to 1/4J(CH) (see Fig. 9), minimum cross-talk can be achieved for all spin systems when different scaling *k* factors are individually applied on each multiplicity (**E**–**G**)

and for a certain heteronucleus, usually backbone CH or NH spin systems. For the first time, we have developed here novel HSQC-IPAP methods to extract valuable information simultaneously for CH_n and NH_n multiplicities in a single NMR experiment. The incorporation of combined advantages associated to time-sharing evolution and IPAP editing do not severely affect the main features of traditional single-nucleus experiments in terms of relative sensitivity and performance (Meissner et al. 1997; Sørensen et al. 1997, 1999; Andersson et al. 1998; Ottiger et al. 1998; Nolis et al. 2006). The time savings and the substantial amount of additional information provided by this methodology can have a significant impact in the development of powerful NMR techniques that might allow complete studies simultaneously on all backbone and side-chain frameworks in small peptides and also labeled proteins. We are also exploring the design of new time-sharing NMR experiments for a broader application to mass-limited and low-concentrated samples as well as to high-throughput structure determination.

Acknowledgments This work was supported by MCYT (project BQU2003-01677). The authors are grateful to the Servei de Ressonància Magnètica Nuclear, UAB, for allocating instrument time to this project and to Dr. W. Bermel for providing us a TS pulse program code. P.N thanks ''Generalitat de Catalunya'' for a predoctoral grant.

References

Andersson P, Weigelt J, Otting G (1998) Spin-state selection filters for the measurement of heteronuclear one-bond coupling constants. J Biomol NMR 12:435–441

Boelens R, Burgering M, Fogh RH and Kaptein R (1994) J Biomol NMR 4:201–213

Carlomagno T, Peti W, Griesinger C (2000) A new method for the simultaneous measurement of magnitude and sign of $^{1}D_{CH}$ and $^{1}D_{HH}$ dipolar couplings in methylene groups. J Biomol NMR 17:99–109

Ding K, Gronenborn AM (2003) Sensitivity-enhanced 2D IPAP, TROSY/anti-TROSY, and E.COSY experiments: Alternatives for measuring dipolar $^{15}N^{1}HN$ couplings. J Magn Reson 163:208–214

Farmer II BT (1991) Simultaneous [^{13}C,^{15}N]-HMQC, A pseudo-triple-resonance Experiment. J Magn Reson 93:635–641

Fehér K, Berger S, Kövér KE (2003) Accurate determination of small one-bond heteronuclear residual dipolar couplings by F1 coupled HSQC modified with a G-BIRD(r) module. J Magn Reson 163:340–346

Frueh DP, Arthanari H, Wagner G (2005) Unambiguous Assignment of NMR Protein Backbone Signals with a Time-shared Triple-resonance Experiment. J Biomol NMR 33:187–196

Giesen AW, Bae LC, Barrett CL, Chyba JA, Chaykovsky MM, Cheng M-C, Murray JH, Oliver EJ, Sullivan SM, Brown JM, Dahlquist FW, Homans SW (2001) Measurement of one-bond $^{1}H\alpha$-$^{13}C\alpha$ couplings in backbone-labelled proteins. J Biomol NMR 19:255–260

Hall JB, Dayie KT, Fushman D (2003) Direct measurement of the ^{15}N CSA/dipolar relaxation interference from coupled HSQC spectra. J Biomol NMR 26:181–186

Hall JB, Fushman D (2003) Direct measurement of the transverse and longitudinal ^{15}N chemical shift anisotropy-dipolar cross-correlation rate constants using ^{1}H-coupled HSQC spectra. Magn Reson Chem 41:837–842

Ishii Y, Markus MA, Tycko R (2001) Controlling residual bipolar couplings in high-resolution NMR of proteins by strain induced alignment in a gel. J Biomol NMR 21:141–151

Kay LE, Keifer P, Saarinen T (1992) Pure absorption gradient-enhanced heteronuclear single-quantum correlation spectroscopy with improved sensitivity. J Am Chem Soc 114:10663–10665

Kim S, Szyperski T (2003) GFT NMR, A new approach to rapidly obtain precise high-dimensional NMR spectral information. J Am Chem Soc 125:1385–1393

Kontaxis G, Bax A (2001) Multiplet component separation for measurement of methyl ^{13}C-^{1}H dipolar couplings in weakly aligned proteins. J Biomol NMR 20:77–82

Kövér KE, Batta G (2004) More line narrowing in TROSY by decoupling of long-range couplings: shift correlation and $^{1}J_{NC}$ coupling constant measurements. J Magn Reson 170:184–190

Mariani M, Tessari M, Boelens R, Vis H, Kaptein R (1994) Assignment of the Protein Backbone from a Single 3D, N-15, C-13, Time-Shared HxyH Experiment. J Magn Reson Series B 104:294–297

Meissner A, Duus JO, Sørensen OW (1997) Integration of spin-state-selective excitation into 2D NMR correlation experiments with heteronuclear ZQ/DQ π rotations for $^{1}J(XH)$-resolved E.COSY-type measurement of heteronuclear coupling constants in proteins. J Biomol NMR 10:89–94

Miclet E, O'Neil-Cabello E, Nikonowicz EP, Live D, Bax A (2003) ^{1}H-^{1}H dipolar couplings provide a unique probe of RNA backbone structure. J Am Chem Soc 125:15740–15741

Miclet E, Williams Jr DC, Clore GM, Bryce DL, Boisbouvier J, Bax A (2004) Relaxation-optimized NMR spectroscopy of methylene groups in proteins and nucleic acids. J Am Chem Soc 126:10560–10570

Nolis P, Espinosa JF, Parella T (2006) Optimum spin-state selection for all multiplicities in the acquisition dimension of the HSQC experiment. J Magn Reson 180:39–50

Ottiger M, Delaglio F, Bax A (1998) Measurement of J and dipolar couplings from simplified two-dimensional NMR spectra. J Magn Reson 131:373–378

Parella T, Gairí M (2004) Simultaneous recording of spin-state-selective NMR spectra for different I_nS spin systems. J Am Chem Soc 126:9821–9826

Permi P (2002) A spin-state-selective experiment for measuring heteronuclear one-bond and homonuclear two-bond couplings from an HSQC-type spectrum. J Biomol NMR 22:27–35

Sattler M, Maurer M, Schleucher J, Griesinger C (1995) A simultaneous ^{15}N,^{1}H and ^{13}C,^{1}H-HSQC with sensitivity enhancement and a heteronuclear echo. J Biomol NMR 5:97–102

Schleucher J, Schwendinger M, Sattler M, Schmidt P, Schedletzky O, Glaser SJ, Sørensen OW, Griesinger C (1994) A general enhancement scheme in heteronuclear multidimensional NMR employing pulsed field gradients. J Biomol NMR 4:301–306

Sørensen MD, Meissner A, Sørensen OW (1997) Spin-state-selective coherence transfer via intermediate states of two-spin coherence in IS spin systems. Application to E.COSY-type measurement of J coupling constants. J Biomol NMR 10:181–186

Sørensen MD, Meissner A, Sørensen OW (1999) ^{13}C natural abundance S^3E and S^3CT experiments for measurement of J coupling constants between $^{13}C^{\alpha}$ or $^{1}H^{\alpha}$ and other protons in a protein. J Magn Reson 137:237–242

Sørensen OW (1990) Aspects and prospects of multidimensional time-domain spectroscopy. J Magn Reson 89:210–216

Szyperski T, Yeh DC, Sukumaran DK, Moseley HN, Montelione GT (2002) Reduced Dimensionality NMR spectroscopy for high-throughput protein resonance assignment. Proc Natl Acad Sci USA 99:8009–8014

Uhrin D, Bramham J, Winder SJ, Barlow PN (2000) Simultaneous CT-^{13}C and VT-^{15}N chemical shift labelling. Application to 3D NOESY-CH_3NH and 3D ^{13}C,^{15}N HSQC-NOESY-CH_3NH. J Biomol NMR 18:253–259